iScience

CellPress
OPEN ACCESS

Article

Artificial nondirectional site-specific recombination systems

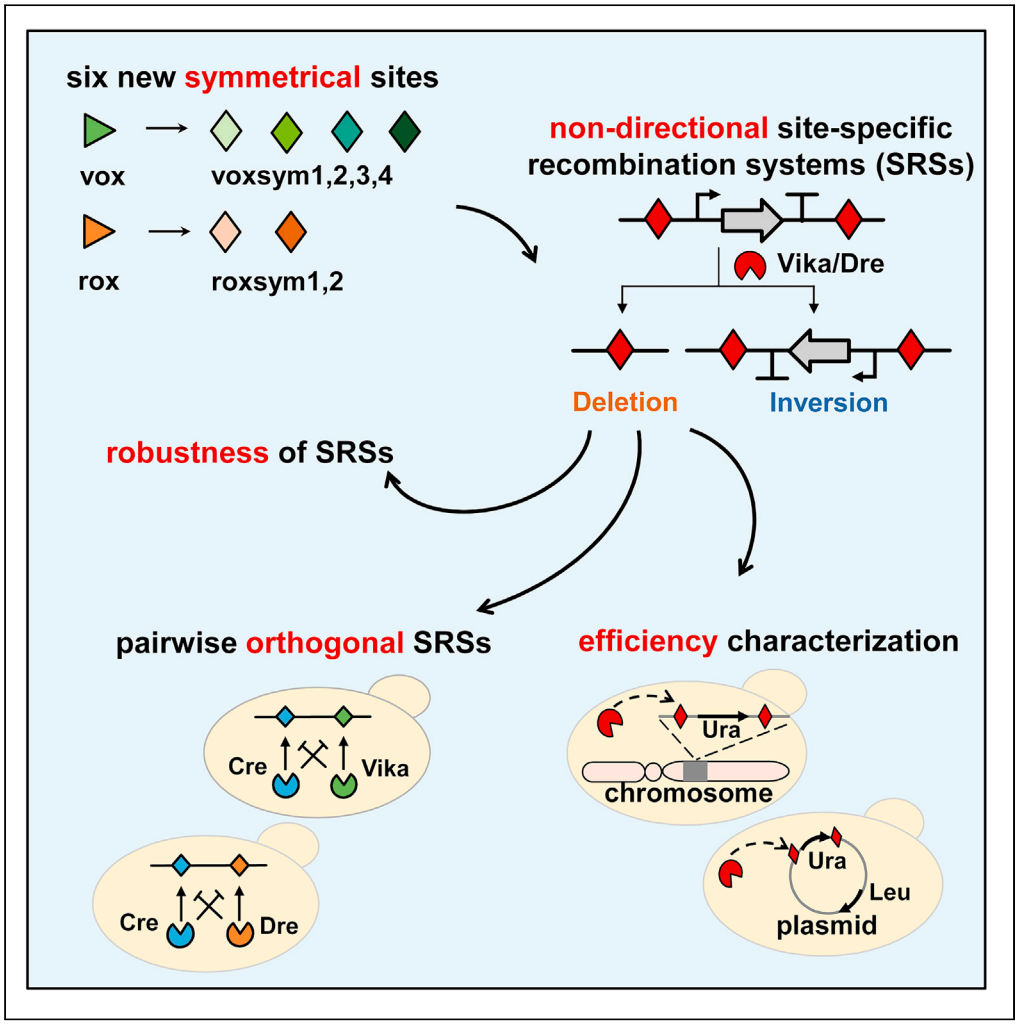

Jun-Yi Wang, Yue-Yang Cao, Ya-Nan Chen, ..., Yi Wu, Bing-Zhi Li, Ying-Jin Yuan

bzli@tju.edu.cn

Highlights

Designed six new artificial nondirectional site-specific recombination systems

Pairwise orthogonal nondirected recombination systems in yeast

The deletion efficiency of systems is far greater than the inversion efficiency

These nondirectional recombination systems were found to be robust

Wang et al., iScience 25, 103716
January 21, 2022
https://doi.org/10.1016/j.isci.2021.103716

iScience

CellPress
OPEN ACCESS

Article

Artificial nondirectional site-specific recombination systems

Jun-Yi Wang,[1,2] Yue-Yang Cao,[1,2] Ya-Nan Chen,[1,2] Xiao-Le Wu,[1,2] Bo-Tao He,[1,2] Si-Yu Zhu,[1,2] Xiao Zhou,[1,2] Yi Wu,[1,2] Bing-Zhi Li,[1,2,3,*] and Ying-Jin Yuan[1,2]

SUMMARY

Site-specific recombination systems (SRSs) are widely used in studies on synthetic biology and related disciplines. Nondirectional SRSs can randomly trigger excision, integration, reversal, and translocation, which are effective tools to achieve large-scale genome recombination. In this study, we designed 6 new nondirectional SRSs named Vika/voxsym1-4 and Dre/roxsym1-2. All 6 artificial nondirectional SRSs were able to generate random deletion and inversion in *Saccharomyces cerevisiae*. Moreover, all six SRSs were orthogonal to Cre/loxPsym. The pairwise orthogonal nondirected SRSs can simultaneously initiate large-scale and independent gene recombination in two different regions of the genome, which could not be accomplished using previous orthogonal systems. These SRSs were found to be robust while working in the cells at different growth stages, as well as in the different spatial structure of the chromosome. These artificial pairwise orthogonal nondirected SRSs offer newfound potential for site-specific recombination in synthetic biology.

INTRODUCTION

Site-specific recombination systems (SRSs) have become important tools in genome engineering. SRS is one of the main approaches in precise genome editing *in vivo*, whereas restriction enzymes and DNA ligases play a major role in manipulating DNA *in vitro*. In addition, many SRSs can function in heterologous organisms where they can be used to manipulate or engineer the genome of heterologous hosts. Site-specific recombinases (SSRs) are mainly divided into tyrosine recombinase and serine recombinase (Brown et al., 2011; Meinke et al., 2016). The lambda integrase (Int), Cre recombinase, and FIP recombinase are common types of tyrosine recombinases, whereas resolvase/invertases such as φC31, γδ, and Tn3 are members of the serine recombinase family (Andrews et al., 1985; Austin et al., 1981; Ausubel, 1974; Nash, 1974; Nash and Robertson, 1981; Volkert and Broach, 1986). The two recombination sites of serine recombinase are different, whereas the two recombination sites of tyrosine are identical. This indicates that recombination based on tyrosine may be reversible in principle, whereas recombination based on serine is unidirectional.

New tyrosine recombinases have been discovered in recent years, such as Dre, VCre, SCre, and Vika, etc. Among them, Dre was the first to be discovered and was closely related to the P1 Cre recombinase, but it had a distinct DNA specificity for a 32 bp DNA site (rox) (Sauer and McDermott, 2004). Next to be discovered were VCre and SCre, which share a lower protein similarity with Cre. VCre originated from plasmid of *Vibrio* sp, whereas SCre was produced from the plasmid of *Shewanella* sp. (Suzuki and Nakayama, 2011). Vika was the latest tyrosine recombinase to be discovered from a degenerate bacteriophage of *Vibrio coralliilyticus,* with a low sequence similarity to other tyrosine recombinases but performs similar functions (Karimova et al., 2013). These recombinases have been demonstrated to be highly specific to their own recombination sites without recombining target sites from other SSRs. The discovery of these new recombinases and recognition sites of various mutations have enhanced the tyrosine recombination system, allowing researchers to accurately modify the genome and develop more complex systems.

The Cre/*loxP* remains the most widely used system on animals, plants, and microorganisms (Gilbertson, 2003; Luo et al., 2020; Song and Palmiter, 2018). Various reactions can be generated depending on the relative orientation of spacers, including recombinase-mediated excision, integration, inversion, and even recombinase-mediated cassette exchange. Furthermore, the recombination site loxPsym of the complete

[1]Frontier Science Center for Synthetic Biology and Key Laboratory of Systems Bioengineering (Ministry of Education), School of Chemical Engineering and Technology, Tianjin University, Tianjin 300072, China

[2]Collaborative Innovation Center of Chemical Science and Engineering (Tianjin), Tianjin University, Tianjin 300072, China

[3]Lead contact

*Correspondence: bzli@tju.edu.cn

https://doi.org/10.1016/j.isci.2021.103716

palindrome can randomly delete or invert the DNA sequence between the sites under the Cre recombinase (Hoess et al., 1986). This system has been used in the international Synthetic Yeast Genome Project, Sc2.0 (Annaluru et al., 2014; Dymond et al., 2011; Mitchell et al., 2017; Richardson et al., 2017; Shen et al., 2017; van der Sloot and Tyers, 2017; Wu et al., 2017; Xie et al., 2017; Zhang et al., 2017) for synthetic chromosome recombinations, offering a system that rearranges the order of genetic information on chromosomes. The LoxPsym-mediated Evolution (SCRaMbLE) system enables quick large-scale genome recombination (Shen et al., 2016), and is able to carry out directed evolution of the genome under selective conditions. Through an in-depth study of the SCRaMbLE system, a more precise control of the system can be realized while related application tools have been developed (Jia et al., 2018; Liu et al., 2018; Shen et al., 2018; Wu et al., 2018). The system has become an effective means to optimize the host, increase product yield, and enhance strain tolerance (Jia et al., 2018; Ma et al., 2019; Wang et al., 2018). Moreover, the SCRaMbLE system has also been used to study synthetic lethal interactions (Wang et al., 2020). With the aforementioned advantages, SCRaMbLE is a useful tool in synthetic biology. More nondirected SRSs would further enable us to investigate key genome issues based on genome synthesis.

This study has created six new artificial nondirected SRSs that can cause random inversion and deletion of the DNA fragment in *S. cerevisiae*. The deletion and inversion efficiency of these SRSs were accurately quantified, and the robustness levels of these SRSs were evaluated. Furthermore, we demonstrated the orthogonality among the six nondirected SRSs and Cre/loxpsym system, which will be applied to synthetic genomes with completed gene clustering.

RESULTS

Development of six new non-directional SRSs

Previous studies have shown that naturally occurring *loxP* sites are asymmetric and can only generate deletions or inversions, whereas the sequence can be deleted and inversed randomly via Cre-mediated recombination among symmetrical synthetic loxPsym sites. The recombination efficiency is comparable to the efficiency among wild-type *loxP* sites (Hoess et al., 1986). We reasoned that completely symmetrical sites can result in an uncertain recombination direction, and it can be deleted or inverted under the action of corresponding recombinase. Four mutant vox sites and two mutant rox sites have been designed, which are all perfect palindromic sequences (Figures 1A and 1B). To verify whether the six nondirectional SRSs can achieve the desired outcome, we inserted the designed recombination sites outside the Ura expression box. Before recombination, primers JYW109 and JYW110 can amplify a 535 bp fragment, but primers JYW109 and JYW111 cannot amplify fragments (primers for characterization of recombination events in this study are listed in Table S1). If the recombination sites are inverted, primers JYW109 and JYW111 can amplify 471 bp fragments, but primers JYW109 and JYW110 cannot amplify fragments. If the recombination sites are deleted, the fragment amplified by primers JYW112 and JYW113 would change from 1,996 bp to 783 bp. The results have shown that the six nondirectional SRSs we developed can be deleted and inverted randomly under the recombinase (Figure 1C). All strains were sequenced to confirm the occurrence of deletion and inversion.

Efficiency of the designed nondirectional SRSs

After verifying that the system we designed can cause random deletion and inversion on the sequence of recombination sites, we quantified the efficiency of these SRSs. The efficiency characterization element consists of an *Ura* expression cassette with recombinase recognition sites on both sides. Here, the deletion and inversion efficiency of the SRSs were calculated by the colony phenotype and two consecutive PCRs (Figure 2A). Different recombinase-mediated recombination reactions, including the same recombinase with different target sites, have different inversion and deletion ratios. With the exception of Dre/roxsym1, the deletion efficiency of all SRSs is far greater than the efficiency of inversion. The deletion efficiency fluctuates between 40% and 65%, whereas the inversion efficiency is less than 10%, which is consistent with previous findings (Hoess et al., 1986). Cre/loxPsym has the lowest inversion efficiency of 2.08%, whereas Dre/roxsym2 has the highest inversion efficiency of 12.93%, which is about six times more than Cre/loxPsym (plasmid). In addition, the general trend of the efficiency of inversion and deletion measured on the chromosome was consistent with the measurement on the plasmid. Most of these SSRs also exhibited less efficiency on chromosomes compared to plasmids, supporting the findings of previous studies (Hochrein et al., 2018) (Figure 2B and Table S2). However, we also found that the total efficiency of deletion and inversion of the Dre/roxsym1 system on the chromosome is a little higher than that on plasmid. However, the specific reason for such performance is still not clear.

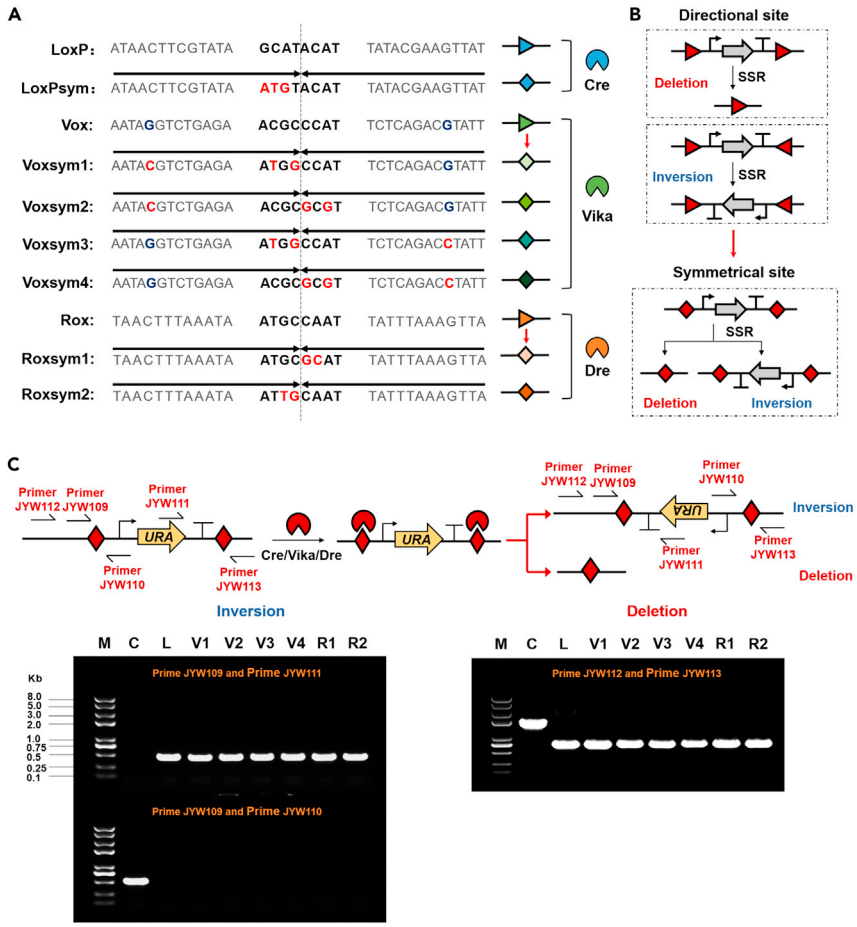

Figure 1. Establishment of non-directional SRSs

(A) Sequence alignment of the directional sites and symmetrical sites. Nucleotides that have changed compared to the directional recombination site are colored in red. Nucleotides in vox that break the perfect palindrome with 13 bp sequences on both sides are colored in blue. Recombination sites with perfect palindrome structure are indicated by arrows.

(B) Schematic diagram on the principles of directional recombination system and nondirectional recombination system.

(C) The nondirectional recombination system can both reverse and delete the sequence among recombination sites. Agarose gel electrophoresis diagram of colony PCR before and after recombination. M, marker; *Trans*2K Plus II DNA Marker, TransGen Biotech, C, Control: before recombination, L, loxPsym, V1, voxsym1, V2, voxsym2, V3, voxsym3, V4, voxsym4, R1, roxsym1, R2, roxsym2.

A genetic AND gate was constructed to enable precise control of the Cre recombinase. The expression of Cre requires the simultaneous addition of galactose and estradiol for full activity (Jia et al., 2018). This strategy allows double regulation on both transcriptional and cellular localization level, which is a good approach for decreasing the leakiness of SSRs. Therefore, all recombinases used in this study were induced and controlled by galactose and estradiol. During the recombination experiments, the strains were cultured on a medium without galactose and estradiol for 8 h as a control group. The same method was used to measure the inversion and deletion efficiency of the control group. Although the expression of the recombinases was already designed as an AND gate, a leakage of recombinase was still observed in Vika/voxsym1-4 recombination systems, but no such leakage was reported in the Cre/loxPsym and Dre/roxsym1-2 recombination systems (Figure S1 and Table S3).

A rapid quantitative efficiency method based on auxotrophic markers and resistance gene

Using phenotypic screening and PCR analysis, we have accurately quantified the efficiency of each SRS. To speed up the quantification of efficiency, we developed a method for rapid quantification of the SRSs based on two auxotrophic markers and one resistance gene. The open reading frame of *Ura* and *Leu*

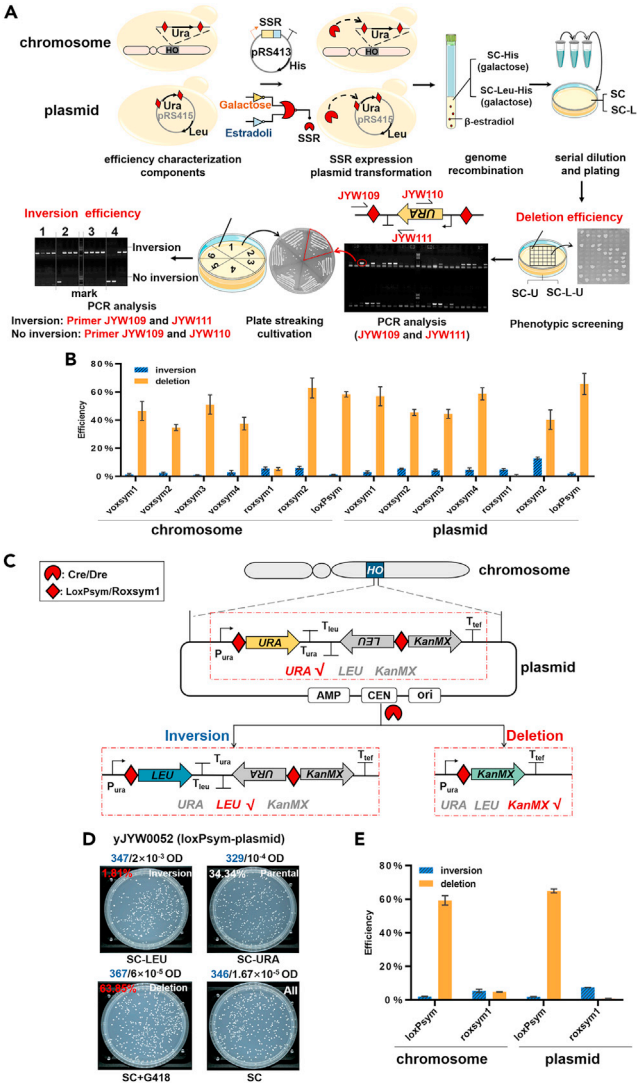

Figure 2. Efficiency of the designed nondirectional SRSs

(A) Experimental flow chart of the efficiency determination of the recombination systems. The efficiency characterization cassettes (symmetrical recombination site-P_{ura}-*Ura*-T_{ura}- symmetrical recombination site) were both integrated into the HO locus of *S. cerevisiae* BY4742 and pRS415 plasmid. The SSR expression plasmid, fused with the EBD binding domain induced by the Gal1 promoter, was transferred to this strain (His was used to screen the SSR expression plasmid). The strain was then induced by galactose and β-estradiol to start the recombination. After 8 h, the genome recombination was completed and the deletion efficiency was first quantified by phenotype. PCR was performed on the colonies without a deletion event. To accurately quantify the inversion efficiency, the strains showing the *Ura* cassette inversion in the first PCR result were streaked and purified. Four single colonies were randomly selected from each purified strain, and PCR was performed again to calculate the final inversion efficiency.

(B) The deletion and inversion efficiency of the recombination systems, error bars indicate SD (n = 3). A total of 96 colonies were screened after each group of recombination experiments.

(C) Schematic overview of rapid quantitative method of recombination system efficiency. The "*Ura*-T_{ura}-T_{leu}-*Leu*" module was randomly deleted or inverted under the action of SSR. Without deletion and inversion, *Ura* gene was expressed, *kanMX* gene was expressed when deletion occurs, and *Leu* gene was expressed when inversion takes place.

(D) A rapid quantitative efficiency method using dilution coating and colony counting. yJYW0052 (Cre, loxPsym, and plasmid) was subjected to recombination experiments under the induction of galactose and β-estradiol. Two OD yeast cells were collected, resuspended in 1 mL water and serially diluted. Finally, an appropriate amount of yeast cells was taken and coated on solid media SC, SC-URA, SC-LEU, and SC+G418 (before the formal verification of efficiency, gradient dilution was used to determine the optimum volume of yeast solution for coating on each plate). The total number of cells spread on each solid plate is marked above each picture. The total number of cells spread on each solid plate and the

Figure 2. *Continued*
count of single colonies on each plate (blue numbers) are marked on the top of each picture. The deletion and inversion efficiency and non-recombination of the Cre/loxPsym recombination system were calculated (numbers in the upper left corner).
(E) The deletion and inversion efficiency of the Cre/loxPsym and Dre/roxsym1 systems on chromosome and plasmid,error bars indicate SD (n = 3). The total number of yeast cells collected in each group of parallel experiments is 2OD.

with their terminators were positioned adjacent to each other and in a convergent direction to make the "*Ura*-T_{ura}-T_{leu}-*Leu*" module. The module was flanked by two identical symmetrical sites, with the *Ura* promoter inserted upstream and open reading frame of *kanMX*, *TEF* terminator placed downstream. Before the recombinant was turned on, the plasmid expressed the *Ura* gene. If the sequence between the recombination sites is deleted, the *kanMX* gene would express, and the *Leu* gene would express if the sequence between the recombination sites is inverted (Figure 2C). Therefore, only the phenotype of the strains can be used to determine whether recombination occurred and the type of recombination.

We used yJYW0052 (Cre, loxPsym, and plasmid) as an illustrative example to quantify the efficiency of the recombination system. After the recombination experiments, 1 mL of the culture was taken to measure the OD_{600} with a spectrophotometer, two OD of yeast cells were then collected and washed three times with water and resuspended into 1 mL water. We diluted the yeast solution into different concentrations to make the number of colonies growing on different agar plates appropriate for our counting (before the formal verification of efficiency, gradient dilution was used to ascertain the optimum volume of yeast solution for coating on each plate). Later, we quantified the inversion and deletion efficiency of the SRSs by counting the number of colonies on different media based on their dilution multiples. There were 347 colonies on SC-LEU agar plate, 329 colonies on SC-URA agar plate, 367 colonies on SC+G418 agar plate, and 346 colonies on SC agar plate. The number of cells spread on SC-LEU, SC-URA, SC+G418, and SC plates are 2×10^{-3}OD, 10^{-4}OD, 6×10^{-5}OD, and 1.67×10^{-5}OD, respectively. The efficiency of deletion and inversion events was calculated based on the total number of coated cells and the colony count on various plates. The deletion efficiency of Cre/loxPsym (chromosome) was 63.85% and an inversion efficiency of 1.81% (Figure 2D and Table S4). The same method was used to determine the recombination efficiency of Cre/loxPsym and Dre/roxsym1 (plasmid and chromosome). Results indicated that the recombination efficiency quantified by this method is identical with the recombination efficiency quantified by colony phenotyping and PCR (Figure 2E).

However, not all the efficiency of SRSs can be quantified using this method. After the plasmid pJYW015 (voxsym2), pJYW016 (voxsym4), pJYW18 (roxsym2), pJYW33 (voxsym1), or pJYW34 (voxsym3) were transformed into BY4742, the colonies could not grow on SC-URA agar plate (Figure S2). We reasoned that the insertion of some recombination sites (voxsym1-4, roxsym2) would result in the downstream open reading frame unable to express. To verify this hypothesis, we inserted these recombination sites between the promoter and start codon of the GFP gene, and checked whether the GFP gene was expressed through a fluorescence microscope. The results showed that the insertion of voxsym1-4 and roxsym2 sites affected the expression of subsequent genes (Figure S3).

Orthogonality among the designed nondirectional SRSs, Cre/loxPsym, and the genomic background

Cre, Vika, and Dre recognize their targets in a highly specific manner and do not cross-react with non-native sites (Karimova et al., 2013; Sauer and McDermott, 2004). However, we still have to verify whether these SRSs remain orthogonal after the recombination sites mutate. We used two auxotrophic markers, *Ura* and *Leu*, to quickly verify the orthogonality of these SSR systems through colony phenotyping and PCR. The *Leu* cassette flanked by two loxPsym sites and the *Ura* cassette flanked by two voxsym1-4/roxsym1-2 sites were inserted into the plasmid containing the *kanMX* resistance gene or the HO locus of *S. cerevisiae* BY4742. Next, the corresponding SSR expression plasmids were transferred into these strains. The *Leu* expression cassette can only be inversed or deleted under the induction of Cre, and the *Ura* expression cassette can only be inversed or deleted under the induction of Vika or Dre, which proved that the Cre/loxpsym recombination system is orthogonal to the Vika/voxsym and Dre/roxsym recombination systems (Figure 3A).

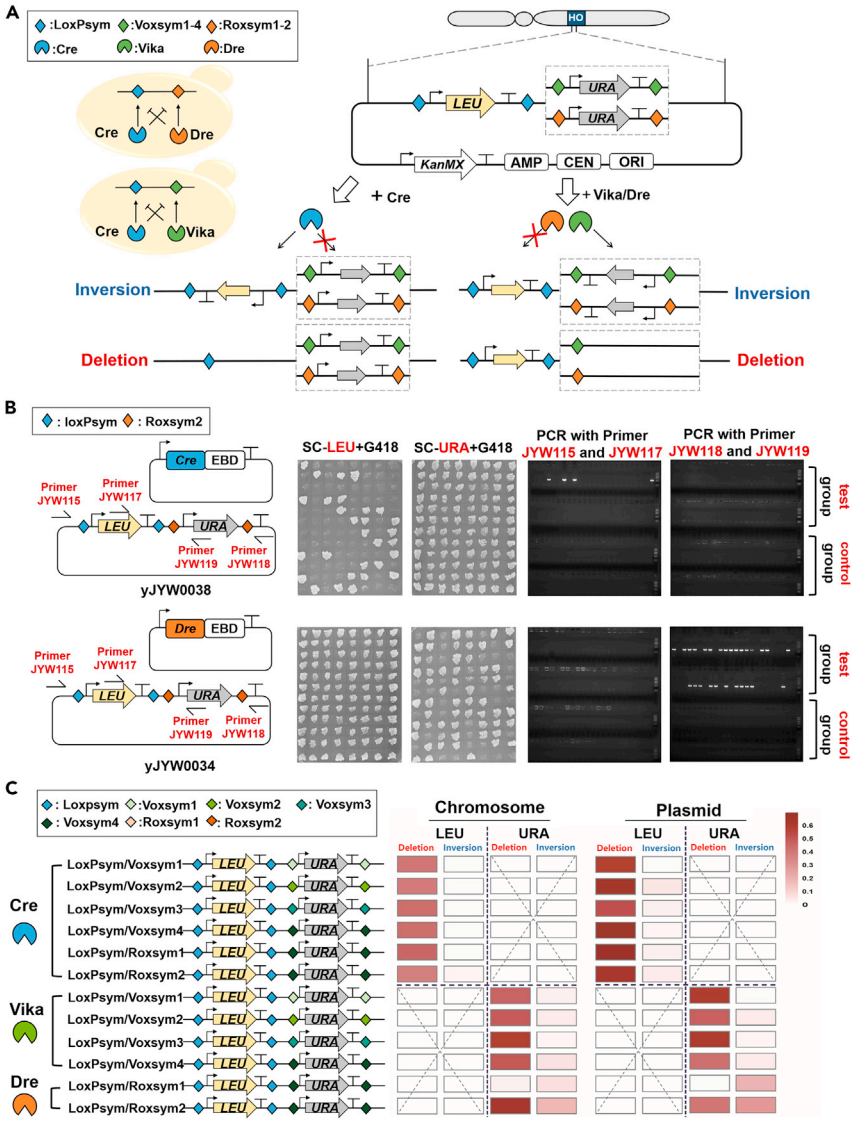

Figure 3. Orthogonality of the designed non-directional SRSs

(A) Schematic overview on the development of orthogonal non-directional SRSs. The *LEU* expression cassette flanked by loxPsym sites can only be deleted or inverted under the action of Cre. The *URA* expression cassette flanked by voxsym1-4 sites can only be deleted or inverted under the action of Vika, while the *URA* expression cassette flanked by roxsym1/2 sites can only be deleted or inverted under the action of Dre.

(B) The orthogonality of Cre/loxPsym and Dre/roxsym2 recombination systems. After the recombination experiment of strain yJYW0038 (Cre, loxpsym, roxsym2) and yJYW0034 (Dre, loxpsym, roxsym2), 96 colonies were randomly selected and spread on SC-URA+G418 and SC-LEU+G418 plates to determine whether the URA and LEU genes were deleted. Two pairs of primers (JYW115, JYW117, and JYW118, JYW119) were then used for colony PCR to determine whether URA and LEU genes were inverted. Galactose and estrogen induction were absent in the control group. A clearer gel electrophoresis image is shown in Figure S4. Primers for characterization of the recombination events in this study are listed in Table S1.

(C) A heatmap was used to represent the orthogonality of Cre/loxPsym and the six non-directional SRSs developed in this study.

We demonstrated the orthogonality of Cre/loxPsym and Dre/roxsym2 recombination system in the recombination experiment of strains yJYW0038 (Cre, loxpsym, roxsym2, and plasmid) and yJYW0034 (Dre, loxpsym, roxsym2, and plasmid) as one such example. After the recombination experiment of strain yJYW0038, 96 colonies were randomly selected and spread on SC-URA+G418 and SC-LEU+G418 plates.

We observed that some single colonies were not able to grow on SC-LEU+G418 agar plate but all colonies grew on the SC-URA+G418 agar plate. However, some single colonies did not grow on SC-URA+G418 agar plates after the recombination experiment of strain yJYW0034, but all colonies were able to grow on SC-LEU+G418 agar plates. An analysis was conducted on whether the *Ura* expression cassette and *Leu* expression cassette were inversed by PCR. After the recombination experiment of strain yJYW0038, only primer JYW115 and primer JYW117 were able to amplify the band of the correct size. Conversely, only primer JYW118 and primer JYW119 amplified the band of the correct size after the recombination experiment of strain yJYW0034. The results showed that 60 of 96 single colonies were not able to grow on the SC-LEU+G418 plate, and the *Leu* gene was inverted in 4 single colonies under the Cre enzyme activity. The deletion efficiency of the Cre/loxPsym was 62.5%, with a 4.2% inversion efficiency. Similarly, the deletion and inversion efficiency of Dre/roxsym2 stood at 40.6% and 28.1%, respectively (Figure 3B). The deletion efficiency of Cre/loxPsym measured in the first part of this paper was 65.6%, whereas inversion efficiency only 2.1%. The deletion and inversion efficiency of Dre/roxsym2 were 40.7% and 12.9%, respectively. The two methods revealed the similar preference of the recombination. The experiments further showed that under the induction of Cre, only the *Leu* expression cassette was inverted or deleted, and only the *Ura* expression cassette was inverted or deleted under the induction of Dre and Vika. We tested the orthogonality among the nondirectional recombination systems developed in this study (Vika/voxsym1-4, Dre/roxsym1-2) and the Cre/loxPsym recombination system. All SRSs in this study were orthogonal to Cre/loxPsym. To provide a more intuitive explanation of their orthogonality, we used a heatmap to demonstrate the inversion and deletion efficiency of them (Figure 3C and Table S5).

Moreover, we assessed whether these SSRs generated ectopic recombination between cryptic recombinase recognition site sequences in the yeast genome. We harvested cells at exponential phase and whole-genome sequencing was performed at BGI (the Beijing Genomics Institute) using the DNBSEQ platform (Wang et al., 2020). Each sample produced an average of 12 Gb of data. The mixed strains after the recombination experiment were selected as test samples, and the strains pJYW016, pJYW019, and pJYW020 without corresponding recombinase were selected as control samples. Compared with the reference genome (*S. cerevisiae* S288C), we got all the single nucleotide polymorphisms (SNPs), insertions, deletions, and structural variations (SVs) of each sample. After ignoring the same insertions, deletions and SVs of all test samples and control samples, only one sample has a suspected SV. Finally, Sanger sequencing was used to further confirm that there was no structural variation at this position. In summary, no off-target or ectopic recombination were found.

Robustness of the designed nondirectional SRSs

To test the robustness of the SRSs, we measured the recombination efficiency of yeast at different growth stages as well as the recombination efficiency of different sites in the *S. cerevisiae* genome. Here, we adopted the method of characterizing efficiency mentioned in the text (colony phenotype and two consecutive PCRs) to quantify the deletion and inversion efficiency. First, we measured the growth curves of strains Yjyw0026 (Cre, loxpsym-chromosome) and Yjyw0024 (Dre, roxsym2-chromosome) on SC-URA-His liquid medium. We selected four representative growth periods: the early stage of the exponential phase (10 h), the middle period of the exponential phase (14 h), the early stage of the plateau phase (20 h), and the middle part of the plateau phase (30 h) to determine the inversion and deletion efficiency of the SRSs. The results showed that the deletion efficiency of Cre/loxPsym fluctuated around 65%, whereas the inversion efficiency fluctuated around 0.5%. The deletion efficiency of Dre/Roxsym2 fluctuated around 65%, and the inversion efficiency fluctuated around 6% (Figure 4A and Table S6). In short, the recombination efficiencies of yeast strains were identical at different growth stages.

Apart from the possibility that the strain activity may have an impact on the efficiency of the SRSs, we speculate that the spatial structure of the chromosome at the recombination site may have a certain impact on the recombination efficiency. Compared with episomal plasmids, these SRSs are more likely to be used in the large-scale recombination of the genome in the future. Therefore, we selected the Dre/roxsym2 system as the object to measure the recombination efficiency at different sites in the genome because it has a higher inversion and deletion efficiency among the SRSs. Researchers have developed a method to globally capture intrachromosomal and interchromosomal interactions, and applied it to generate a three-dimensional model of the haploid genome of *S. cerevisiae*. They established yeast genome architecture features using interactions from the *HindIII* libraries, and verified them with interactions from the *EcoRI* libraries (Duan et al., 2010). We calculated the sum of intrachromosomal and interchromosomal interactions at all points in the *HindIII* libraries, and 2 sites with strong interaction

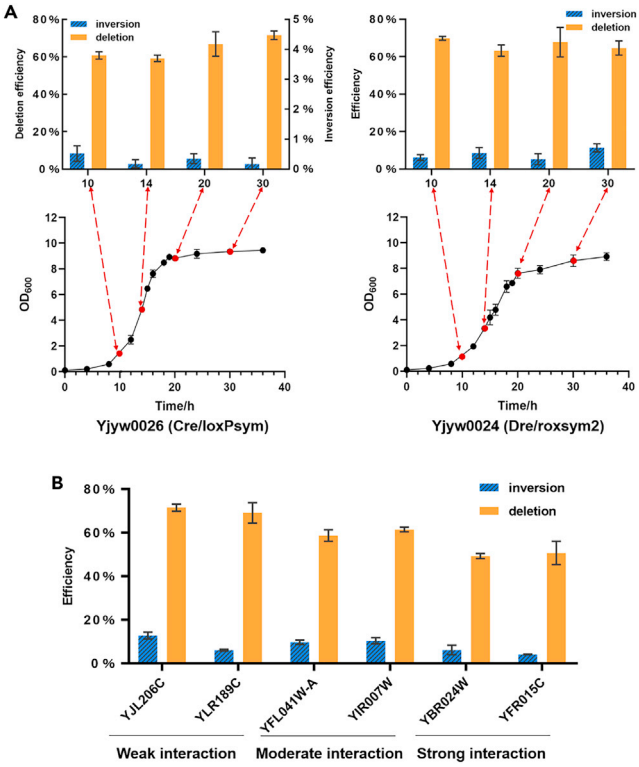

Figure 4. Robustness of the designed non-directional SRSs

(A) The effect of the growth stages on the efficiency of the designed non-directional SRSs. We quantified the recombination efficiency of strains at different stages under the Cre/loxPsym and Dre/roxsym2 systems. As the inversion efficiency of the Cre/loxPsym system is too low, we used a dual axis to express the system's deletion (left axis) and inversion efficiency (right axis).Error bars indicate SD (n = 3).

(B) The effect of chromosome spatial structure on the efficiency of the recombination system. We selected 6 sites on the genome with different interaction strengths to quantify the recombination efficiency of the Dre/roxsym2 system.Error bars indicate SD (n = 3).

were selected based on the results, along with 2 sites of moderate interaction and 2 sites with weak interaction in the genome to quantify the efficiency of the SRSs (Table S7). The deletion efficiency of the Dre/roxsym2 recombination system on the genome fluctuated at 60%, whereas the inversion efficiency fluctuated at 6%. However, the efficiency of the SRSs decreases when the tightness of the chromosomal structures increases at the site of action (Figure 4B and Table S6).

DISCUSSION

We designed six new artificial nondirected SRSs that can cause random inversion and deletion of the DNA fragments. Furthermore, we developed two different methods to accurately quantify the deletion and inversion efficiency of these SRSs. The quantification of the efficiency serves as a reference for the selection of nondirected SRSs in future research.

Most of the previous studies characterized the efficiency of the recombination system by quantifying the deletion efficiency of fragments between two recombination sites in the same direction. They used antibiotic resistance genes, blue-white class screening, auxotrophic markers or fluorescent proteins to quantify the deletion efficiency of SRSs in mammalian, human, and mouse cells (Buchholz et al., 1998; Hoess et al., 1986; Karimova et al., 2013; Lin et al., 2015; Zhang et al., 2019). In this study, we quantified not only the deletion efficiency of the SRSs but also their inversion efficiency. Shen et al. conducted deep sequencing of 64 *synIXR* SCRaMbLE strains and revealed 156 deletions, 89 inversions, 94 duplications, and 55 additional complex recombinations (Shen et al., 2016), which were somewhat different from the efficiency we quantified. The deep sequencing method of SCRaMbLE strains ignored the death of the strains because of the

deletion of essential genes, resulting in the quantified deletion efficiency being lower than the actual situation. To accurately quantify the efficiency of the SRSs, we used the auxotrophic markers to quantify the deletion efficiency of the recombination system through the phenotype of the strain. Colony PCR was then used to identify whether the fragments between recombination sites were inverted. Through this method, we accurately quantified the efficiency of Cre/loxPsym and the six nondirected SRSs developed in this study on the genome and episomal plasmid. The method, based on cell phenotype and colony PCR, is universal and applicable to all nondirected SRSs in quantifying their deletion and inversion efficiency.

We developed a method to speed up the quantifying of the SRSs' efficiency based on two auxotrophic markers and a resistance gene. Fluorescent proteins are often used to characterize the inversion of the fragments between two recombination sites (Yang et al., 2014; Zhao et al., 2019). Furthermore, a reporter of SCRaMbLEd cells was constructed based on a loxP-mediated switch of two auxotrophic markers (Luo et al., 2018). The method of quantifying efficiency proposed in this study added a resistance gene to characterize the deletion of the DNA fragments. To reduce the influence of recombinase recognition sites on gene expression, the resistance gene was inserted at the front of the initiation codon. Three different phenotypes of cells were used to characterize the DNA fragments among recombination sites that were not recombined, or were deleted and inverted, which made it very fast and convenient to quantify the efficiency of the recombination system. Using this method, we completed the quantification of the efficiency of the Cre/loxPsym and Dre/roxsym1 recombination systems. A comparison of the quantified efficiency using the two different measurement methods can further prove the accuracy of our quantified efficiency.

Although the recombination sites have been inserted at the front of the initiation codon, the subsequent gene expression was still affected. We reasoned that the inserted site is a complete palindromic sequence, which forms a perfect hairpin and affects the subsequent gene expression. Previous studies have shown that the stability of the hairpin structure is related to the enthalpy of the DNA sequence. The higher the enthalpy, the more stable the hairpin structure (Senior et al., 1988). The difference in enthalpy between the recognition sites may result in a different degree of influence on subsequent gene expression. We used Vector NTI (Li and Moriyama, 2004) to analyze the enthalpy of loxPsym, voxsym1-4, roxsym1, and roxsym2. The enthalpy values of loxPsym and roxsym1 were found to be lower than those of voxsym1-4 and roxsym2, which are consistent with our hypothesis (Table S8).

The orthogonality of different SRSs is a key parameter for the complex design of the artificial genome. We explored the orthogonality among the six new nondirectional SRSs and Cre/loxPsym. Both the Dre/rox and Vika/vox recombination systems were found to have good orthogonality with the Cre/*loxP* system (Karimova et al., 2013; Sauer and McDermott, 2004). In addition the Vika/vox and Cre/loxPsym systems have also been proved to be pairwise orthogonal in *S. cerevisiae* (Lin et al., 2015). These orthogonal directed SRSs are often combined with various Boolean logic operations to accurately achieve the activation and inactivation of gene expression, or to precisely define the roles of specific cell types (Fenno et al., 2014). Because of the orthogonality of Vika/vox and Cre/loxPsym, Vika/vox can be used for the deletion of genes in synthetic yeast (Lin et al., 2015; Wang et al., 2020). However, the pairwise orthogonal nondirected SRSs constructed in this study can simultaneously initiate large-scale and independent gene recombination in two different regions of the genome, which cannot be accomplished by the previous orthogonal systems. With the continuous development of synthetic biology, the clustering and recombination of synthetic gene modules are gradually being tried (Hutchison et al., 2016; Wang et al., 2020). Among these modules, our pairwise orthogonal non-directed SRSs can be applied.

Robustness is a major feature of biological systems that ensures the system's functions are maintained despite external and internal perturbations. Previous studies have shown that the recombination efficiency of the tyrosine recombination system in *Escherichia coli, S. cerevisiae* and some mammals maintain at a relatively high level, which suggests that tyrosine SRSs are a robust genomic modification tool (Anastassiadis et al., 2009; Karimova et al., 2013; Meinke et al., 2016; Sauer and McDermott, 2004). However, studies were not done on the impact of the growth period and chromosome structure of the strain on the recombination efficiency used in the experiment. Our experimental results further prove the robustness of the tyrosine recombination system: the efficiency of the system was not affected by the growth period of the strain. When the system acts on different sites in the genome, it will be slightly affected by the 3D structure of the chromosome. The areas where the chromosome structure is tight, the steric hindrance is greater, result in lower efficiency of recombinase compared to areas

with loose chromosomes. However, the tyrosine SSRs such as Cre, Dre, and Vika do not require accessory proteins to initiate the recombination reaction. Once the synaptic tetramer structure of the SSR/DNA complex is formed, no large protein–protein or protein–DNA arrangements are required to trigger recombination (Meinke et al., 2016). Therefore, the 3D structure of the chromosome only has a slight effect on the efficiency of these SRSs. Overall, the efficiency of the SRSs is still very robust.

In conclusion, we developed six newnon-directed SRSs: Vika/voxsym1-4, Dre/roxsym1, and Dre/roxsym2, all of which were proven to be orthogonal to the Cre/loxPsym system. The combination of these systems with the Cre/loxPsym will serve as powerful orthogonal tools for large-scale genome recombination, especially for modularized synthetic genomes. In this paper, we have also performed a comprehensive characterization of the efficiency, orthogonality, and robustness of these SRSs, providing a better understanding of the tyrosine recombination system and further promoting its application in synthetic biology.

Limitations of the study

The method proposed in this study to quantify the efficiency of SRSs based on two auxotrophic markers and a resistance gene is a quick and convenient method. However, inhibition of the inserted recombination sites on the expression of its downstream gene should be further investigated. In the future, these recombination sites can be moved to the suitable loci upstream of the start codon to reduce hindrance to downstream gene expression. At present, only the pairwise orthogonal nondirectional recombination system was constructed. In the future, a nondirected recombination system containing three or more orthogonal recombinases can be constructed, which is suitable for multi-module synthetic genomes.

STAR★METHODS

Detailed methods are provided in the online version of this paper and include the following:

- KEY RESOURCES TABLE
- RESOURCE AVAILABILITY
  - Lead contact
  - Materials availability
  - Data and code availability
- EXPERIMENTAL MODEL AND SUBJECT DETAILS
- METHOD DETAILS
  - Construction of plasmids
  - Yeast transformation and assembly
  - Recombination experiments
  - Verification of orthogonality
  - Growth curve assay
- QUANTIFICATION AND STATISTICAL ANALYSIS
  - Quantification of recombination efficiency
  - Rapid quantification of recombination efficiency

SUPPLEMENTAL INFORMATION

Supplemental information can be found online at https://doi.org/10.1016/j.isci.2021.103716.

ACKNOWLEDGMENTS

We would like to express our appreciation to Chao Yuan from Tianjin Medical University for his help in creating the heat map in the orthogonality verification of the nondirectional SRSs. This work was supported by the National Key Research and Development Program of China (2018YFA0900100), Tianjin Fund for Distinguished Young Scholars (19JCJQJC63300), and National Natural Science Foundation of China (21621004).

AUTHOR CONTRIBUTIONS

B.Z.L. and Y.J.Y. conceived the overall project, while J.Y.W., X.L.W., and B.Z.L., designed the experiments. J.Y.W., Y.Y.C., Y.N.C., B.T.H., and S.Y.Z., performed the experiments, and J.Y.W., Y.Y.C., Y.N.C., and B.Z.L. analyzed the data and discussed the results. J.Y.W. wrote the manuscript, while Y.W., X.Z., and B.Z.L. edited the manuscript, with input from all authors. B.Z.L. supervised all aspects of the study.

DECLARATION OF INTERESTS

The authors declare no competing interests.

Received: June 3, 2021
Revised: October 23, 2021
Accepted: December 29, 2021
Published: January 21, 2022

REFERENCES

Anastassiadis, K., Fu, J., Patsch, C., Hu, S., Weidlich, S., Duerschke, K., Buchholz, F., Edenhofer, F., and Stewart, A.F. (2009). Dre recombinase, like Cre, is a highly efficient site-specific recombinase in *E-coli*, mammalian cells and mice. Dis. Models Mech. *2*, 508–515.

Andrews, B.J., Proteau, G.A., Beatty, L.G., and Sadowski, P.D. (1985). The FLP recombinase of the 2 micron circle DNA of yeast: interaction with its target sequences. Cell *40*, 795–803.

Annaluru, N., Muller, H., Mitchell, L.A., Ramalingam, S., Stracquadanio, G., Richardson, S.M., Dymond, J.S., Kuang, Z., Scheifele, L.Z., Cooper, E.M., et al. (2014). Total synthesis of a functional designer eukaryotic chromosome. Science *344*, 55–58.

Austin, S., Ziese, M., and Sternberg, N. (1981). A novel role for site-specific recombination in maintenance of bacterial replicons. Cell *25*, 729–736.

Ausubel, F.M. (1974). Radiochemical purification of bacteriophage lambda integrase. Nature *247*, 152–154.

Brown, W.R.A., Lee, N.C.O., Xu, Z., and Smith, M.C.M. (2011). Serine recombinases as tools for genome engineering. Methods *53*, 372–379.

Buchholz, F., Angrand, P.O., and Stewart, A.F. (1998). Improved properties of FLP recombinase evolved by cycling mutagenesis. Nat. Biotechnol. *16*, 657–662.

Duan, Z., Andronescu, M., Schutz, K., McIlwain, S., Kim, Y.J., Lee, C., Shendure, J., Fields, S., Blau, C.A., and Noble, W.S. (2010). A three-dimensional model of the yeast genome. Nature *465*, 363–367.

Dymond, J.S., Richardson, S.M., Coombes, C.E., Babatz, T., Muller, H., Annaluru, N., Blake, W.J., Schwerzmann, J.W., Dai, J., Lindstrom, D.L., et al. (2011). Synthetic chromosome arms function in yeast and generate phenotypic diversity by design. Nature *477*, 471–476.

Fenno, L.E., Mattis, J., Ramakrishnan, C., Hyun, M., Lee, S.Y., He, M., Tucciarone, J., Selimbeyoglu, A., Berndt, A., Grosenick, L., et al. (2014). Targeting cells with single vectors using multiple-feature Boolean logic. Nat. Methods *11*, 763–772.

Gibson, D.G. (2011). Enzymatic assembly of overlapping DNA fragments. In Synthetic Biology, Pt B: Computer Aided Design and DNA Assembly, *498*, C. Voigt, ed (Academic Press Ltd-Elsevier Science Ltd), pp. 349–361.

Gilbertson, L. (2003). Cre-lox recombination: Cre-ative tools for plant biotechnology. Trends Biotechnol. *21*, 550–555.

Hochrein, L., Mitchell, L.A., Schulz, K., Messerschmidt, K., and Mueller-Roeber, B. (2018). L-SCRaMbLE as a tool for light-controlled Cre-mediated recombination in yeast. Nat. Commun. *9*, 1931.

Hoess, R.H., Anna, W., and Kenneth, A.J.N.A.R. (1986). The role of the loxP spacer region in P1 site-specific recombination. Nucleic Acids Res. *14*, 2287–2300.

Hutchison, C.A., III, Chuang, R.-Y., Noskov, V.N., Assad-Garcia, N., Deerinck, T.J., Ellisman, M.H., Gill, J., Kannan, K., Karas, B.J., Ma, L., et al. (2016). Design and synthesis of a minimal bacterial genome. Science *351*, aad6253.

Jia, B., Wu, Y., Li, B.-Z., Mitchell, L.A., Liu, H., Pan, S., Wang, J., Zhang, H.-R., Jia, N., Li, B., et al. (2018). Precise control of SCRaMbLE in synthetic haploid and diploid yeast. Nat. Commun. *9*, 1933.

Karimova, M., Abi-Ghanem, J., Berger, N., Surendranath, V., Pisabarro, M.T., and Buchholz, F. (2013). Vika/vox, a novel efficient and specific Cre/loxP-like site-specific recombination system. Nucleic Acids Res. *41*, e37.

Li, G.Q., and Moriyama, E.N. (2004). Vector NTI, a balanced all-in-one sequence analysis suite. Brief. Bioinform. *5*, 378–388.

Lin, Q., Qi, H., Wu, Y., and Yuan, Y. (2015). Robust orthogonal recombination system for versatile genomic elements rearrangement in yeast *Saccharomyces cerevisiae*. Sci. Rep. *5*, 15249.

Liu, W., Luo, Z., Wang, Y., Pham, N.T., Tuck, L., Perez-Pi, I., Liu, L., Shen, Y., French, C., Auer, M., et al. (2018). Rapid pathway prototyping and engineering using *in vitro* and *in vivo* synthetic genome SCRaMbLE-in methods. Nat. Commun. *9*, 1936.

Luo, L., Ambrozkiewicz, M.C., Benseler, F., Chen, C., Dumontier, E., Falkner, S., Furlanis, E., Gomez, A.M., Hoshina, N., Huang, W.-H., et al. (2020). Optimizing nervous system-specific gene targeting with Cre driver lines: prevalence of germline recombination and influencing factors. Neuron *106*, 37–65.

Luo, Z., Wang, L., Wang, Y., Zhang, W., Guo, Y., Shen, Y., Jiang, L., Wu, Q., Zhang, C., Cai, Y., and Dai, J. (2018). Identifying and characterizing SCRaMbLEd synthetic yeast using ReSCuES. Nat. Commun. *9*, 1930.

Ma, L., Li, Y., Chen, X., Ding, M., Wu, Y., and Yuan, Y.-J. (2019). SCRaMbLE generates evolved yeasts with increased alkali tolerance. Microb. Cell Factories *18*, 52.

Meinke, G., Bohm, A., Hauber, J., Pisabarro, M.T., and Buchholz, F. (2016). Cre recombinase and other tyrosine recombinases. Chem. Rev. *116*, 12785–12820.

Mitchell, L.A., Wang, A., Stracquadanio, G., Kuang, Z., Wang, X., Yang, K., Richardson, S., Martin, J.A., Zhao, Y., Walker, R., et al. (2017). Synthesis, debugging, and effects of synthetic chromosome consolidation: synVI and beyond. Science *355*, eaaf4831.

Nash, H.A. (1974). Purification of bacteriophage lambda Int protein. Nature *247*, 543–545.

Nash, H.A., and Robertson, C.A. (1981). Purification and properties of the *Escherichia coli* protein factor required for lambda integrative recombination. J. Biol. Chem. *256*, 9246–9253.

Richardson, S.M., Mitchell, L.A., Stracquadanio, G., Yang, K., Dymond, J.S., DiCarlo, J.E., Lee, D., Huang, C.L.V., Chandrasegaran, S., Cai, Y., et al. (2017). Design of a synthetic yeast genome. Science *355*, 1040–1044.

Sauer, B., and McDermott, J. (2004). DNA recombination with a heterospecific Cre homolog identified from comparison of the pac-c1 regions of P1-related phages. Nucleic Acids Res. *32*, 6086–6095.

Senior, M.M., Jones, R.A., and Breslauer, K.J. (1988). Influence of loop residues on the relative stabilities of DNA hairpin structures. Proc. Natl. Acad. Sci. U S A *85*, 6242–6246.

Shen, M.J., Wu, Y., Yang, K., Li, Y., Xu, H., Zhang, H., Li, B.-Z., Li, X., Xiao, W.-H., Zhou, X., et al. (2018). Heterozygous diploid and interspecies SCRaMbLEing. Nat. Commun. *9*, 1934.

Shen, Y., Stracquadanio, G., Wang, Y., Yang, K., Mitchell, L.A., Xue, Y., Cai, Y., Chen, T., Dymond, J.S., Kang, K., et al. (2016). SCRaMbLE generates designed combinatorial stochastic diversity in synthetic chromosomes. Genome Res. *26*, 36–49.

Shen, Y., Wang, Y., Chen, T., Gao, F., Gong, J., Abramczyk, D., Walker, R., Zhao, H., Chen, S., Liu, W., et al. (2017). Deep functional analysis of synII, a 770-kilobase synthetic yeast chromosome. Science *355*, eaaf4791.

Song, A.J., and Palmiter, R.D. (2018). Detecting and avoiding problems when using the Cre-lox system. Trends Genet. *34*, 333–340.

Suzuki, E., and Nakayama, M. (2011). VCre/VloxP and SCre/SloxP: new site-specific recombination systems for genome engineering. Nucleic Acids Res. *39*, e49.

van der Sloot, A., and Tyers, M. (2017). Synthetic genomics: rewriting the genome chromosome by chromosome. Mol. Cell *66*, 441–443.

Volkert, F.C., and Broach, J.R. (1986). Site-specific recombination promotes plasmid amplification in yeast. Cell *46*, 541–550.

Wang, J., Jia, B., Xie, Z., Li, Y., and Yuan, Y. (2018). Improving prodeoxyviolacein production via multiplex SCRaMbLE iterative cycles. Front. Chem. Sci. Eng. *12*, 806–814.

Wang, P., Xu, H., Li, H., Chen, H., Zhou, S., Tian, F., Li, B.-Z., Bo, X., Wu, Y., and Yuan, Y.-J. (2020). SCRaMbLEing of a synthetic yeast chromosome with clustered essential genes reveals synthetic lethal interactions. ACS Synth. Biol. *9*, 1181–1189.

Wu, Y., Li, B.-Z., Zhao, M., Mitchell, L.A., Xie, Z.-X., Lin, Q.-H., Wang, X., Xiao, W.-H., Wang, Y., Zhou, X., et al. (2017). Bug mapping and fitness testing of chemically synthesized chromosome X. Science *355*, aaf4706.

Wu, Y., Zhu, R.-Y., Mitchell, L.A., Ma, L., Liu, R., Zhao, M., Jia, B., Xu, H., Li, Y.-X., Yang, Z.-M., et al. (2018). *In vitro* DNA SCRaMbLE. Nat. Commun. *9*, 1935.

Xie, Z.-X., Li, B.-Z., Mitchell, L.A., Wu, Y., Qi, X., Jin, Z., Jia, B., Wang, X., Zeng, B.-X., Liu, H.-M., et al. (2017). "Perfect" designer chromosome V and behavior of a ring derivative. Science *355*, eaaf4704.

Xu, H., Han, M., Zhou, S., Li, B.Z., Wu, Y., and Yuan, Y.J. (2020). Chromosome drives via CRISPR-Cas9 in yeast. Nat. Commun. *11*, 4344. https://doi.org/10.1038/s41467-020-18222-0.

Yang, L., Nielsen, A.A.K., Fernandez-Rodriguez, J., McClune, C.J., Laub, M.T., Lu, T.K., and Voigtwill, C.A. (2014). Permanent genetic memory with > 1-byte capacity. Nat. Methods *11*, 1261–1266.

Zhang, W., Zhao, G., Luo, Z., Lin, Y., Wang, L., Guo, Y., Wang, A., Jiang, S., Jiang, Q., Gong, J., et al. (2017). Engineering the ribosomal DNA in a megabase synthetic chromosome. Science *355*, eaaf3981.

Zhang, Z., Lu, Y., Chi, Z., Liu, G.-L., Jiang, H., Hu, Z., and Chi, Z.-M. (2019). Genome editing of different strains of Aureobasidium melanogenum using an efficient Cre/loxp site-specific recombination system. Fungal Biol. *123*, 723–731.

Zhao, J., Pokhilko, A., Ebenhoeh, O., Rosser, S.J., and Colloms, S.D. (2019). A single-input binary counting module based on serine integrase site-specific recombination. Nucleic Acids Res. *47*, 4896–4909.

STAR★METHODS

KEY RESOURCES TABLE

REAGENT or RESOURCE	SOURCE	IDENTIFIER
Bacterial and virus strains		
Escherichia coli: DH5α	TSINGKE	CAS SW-c0396TSV-A07
Chemicals, peptides, and recombinant proteins		
*Trans*2K Plus II DNA Marker	TransGen Biotech	Cat# BM121-01
*Not*I-HF	NEB	Cat# R3189L
*Sal*I-HF	NEB	Cat# R3138L
*Bam*HI-HF	NEB	Cat# R3136L
NEBuilder® HiFi DNA Assembly Master Mix	NEB	Cat# E2621L
T4 DNA Ligase	NEB	Cat# M0202L
Phanta Max Super-Fidelity DNA Polymerase	Vazyme	Cat# P505-d1
2 × Rapid Taq Master Mix	Vazyme	Cat# P222-01
Tryptone	OXOID	Cat# LP0042B
Yeast extract	OXOID	Cat# LP0021B
NaCl	Sigma-Aldrich	CAS 7647-14-5
Yeast Nitrogen Base	Genview	Cat# KY373-100G
Agar	DingGuo	Cat# DH010-1.1
D-(+)-Galactose	aladdin	CAS 59-23-4
β-estradiol	Sigma-Aldrich	CAS 50-28-2
Lithium acetate dihydrate	Sigma-Aldrich	CAS 6108-17-4
Polyethylene glycol	Sigma-Aldrich	CAS 25322-68-3
Dimethyl sulfoxide	Sigma-Aldrich	CAS 67-68-5
Calcium chloride dihydrate	aladdin	CAS10035-04-8
Critical commercial assays		
AxyPrep Plasmid Miniprep Kit	Axygen	Cat# AP-MN-P-250
AxyPrep DNA Gel Extraction Kit	Axygen	Cat# AP-GX-250
Experimental models: Organisms/strains		
S. cerevisiae: Strain background: BY4742	ATCC	74,224
Oligonucleotides		
For all primers used in this study	See Tables S1 and S11	N/A
Recombinant DNA		
Plasmids constructed in this study	See Table S10	N/A
Strains constructed in this study	See Table S9	N/A
Software and algorithms		
Prism 8	GraphPad	https://www.graphpad.com/
SnapGene®4.2.4	SnapGene	https://www.snapgene.com/

RESOURCE AVAILABILITY

Lead contact

Further information and requests for code should be directed to the lead contact Bing-Zhi Li (bzli@tju.edu.cn).

Materials availability

The study did not generate any materials.

Data and code availability

All data reported in this paper will be shared by the lead contact upon request.

This paper does not report original code.

Any additional information required to reanalyze the data reported in this paper is available from the lead contact upon request.

EXPERIMENTAL MODEL AND SUBJECT DETAILS

All *S. cerevisiae* strains used in this study were derived from the BY4742 background strain (*MATα* his3Δ1 leu2Δ0 lys2Δ0 ura3Δ0). *E. coli* strain DH5α grown in Luria Broth (LB) media was used for cloning purposes. *S. cerevisiae* BY4742 was used as the initial host for DNA assembly and transformation in this study. All yeast strains are described in Table S9. Yeast strains were cultured in yeast peptone dextrose (YPD) medium or synthetic complete (SC) dropout medium supplemented with amino acids and/or drugs.

METHOD DETAILS

Construction of plasmids

Recombination efficiency characterization plasmids were based on the pRS415 vector and developed by inserting efficiency characterization cassettes using *Sal*I and *Bam*HI restriction enzymes (NEB). The efficiency characterization cassettes were generated using overhang primers to add a symmetric recombination site (loxPsym, roxsym1-2, voxsym1-4) to both sides of the Ura cassette. Symmetric recombination sites were developed from mutations in vox and rox using chemically synthesized oligonucleotides.

The SSRs expression plasmids (*GAL1*p-Vika/Dre-EBD-*CYC1*t) were assembled into pRS413 linearized by *Bam*HI and *Not*I (NEB) through overlap-based DNA assembly methods. *Dre* was identified from phage D6 and the coding sequence was obtained from the GenBank database: AY753669 (Sauer and McDermott, 2004), purchased as gBlock from TSINGKE Biological Technology.

The plasmids for rapid characterization of recombination efficiency and construction of one linearization vector involved the *Ura* promoter and three PCR-amplified DNA fragments: *Ura* and its terminator with a symmetric recombination site on the left, the inverted *Leu* and its terminator with a symmetric recombination site on the right and *KanMX* with *TEF* terminator. All three PCR products were inserted via Gibson assembly into the linearized vector (Gibson, 2011).

To construct orthogonal verification plasmids, the linearization vector-containing the *Ura* cassette flanked by two identical symmetric recombination sites (voxsym2/voxsym4/roxsym1/roxsym2)-was PCR amplified from recombination efficiency characterization plasmids. The *Leu* cassette was flanked by two loxPsym sites and the *KanMX* cassette was also obtained through PCR. The two PCR products were inserted via Gibson assembly into the linearized vector. All the plasmids and primers for plasmids or strains construction used in this study are described in Table S10 and Data S1.

Yeast transformation and assembly

S. cerevisiae transformations were carried out using standard lithium acetate procedures in this study: The yeast colonies were incubated in 5 mL of YPD overnight at 30°C with shaking at 220 rpm. Later, 200 μL of the culture was transferred to 5 mL of YPD (30°C, 220 rpm). When the OD600 reached 0.4 ± 0.6, 1 mL of cells was collected and washed with sterile H2O. The cells were then resuspended in 1 mL of 0.1 M LiOAc solution and placed on ice for 5 min. Moreover, 620 μL of polyethylene glycol (PEG) 3350, 150 μL sterile H2O, 40 μL of salmon DNA and 90 μL of 1 M LiOAc were mixed together, which served as transformation buffer. The salmon DNA was preheated at 100°C for 10 min and then cooled on ice. Pretreated cells (100 μL) were added and mixed in the transformation buffer, after which they were cultured at 30°C for 30 min. The culture was then combined with dimethyl sulfoxide (DMSO) and heat-shocked at 42°C for 20 min. The solution was centrifuged at 4,000 g for 5 min, and the supernatant was discarded. The cells were recovered and resuspended in 500 μL 5 mM $CaCl_2$ for 5 min, and plated onto the corresponding selective media (Xu et al., 2020).

The overlap extension PCR was used to build the DNA cassette flanked by 500 bp genomic homology region. The PCR products were then transformed into BY4742 to complete the integration. After the appropriate selective media was chosen, PCR and sequencing were used to confirm the integrants.

Recombination experiments

Single colonies were chosen and inoculated in 3 mL liquid SC-URA-HIS-Leu (SC-URA-HIS) media and cultured overnight at 30°C on a rotary shaker (220 rpm). Cultures were washed twice with ddH_2O and re-inoculated to obtain an OD_{600} of 1.0 in 2% galactose SGal-His-Leu (SGal-His) medium containing 1 μM β-estradiol (Control group: Cultures were washed twice with ddH_2O and re-inoculated to obtain an OD_{600} of 1.0 in 2% glucose SC-HIS-LEU (SC-His) medium without β-estradiol). The cultures were incubated at 30°C with shaking at 220 rpm for 8 h to turn on SSRs activity in the cells and begin the recombination progress. Cultures were spun down at 4,000 × *g* for 5 min and washed three times with water to wash out galactose and β-estradiol while cells underwent serial dilution and were plated on solid SC-LEU (SC) medium for 2 days at 30°C.

Verification of orthogonality

Following the recombination experiment, 96 colonies were randomly selected and spread on both SC-URA (SC-URA+G418) and SC-LEU (SC-LEU+G418) plates overnight. The deletion efficiency of *Ura/Leu* cassette was quantified by counting the number of colonies which could not grow on SC-URA (SC-URA+G418)/SC-LEU (SC-LEU+G418) plate. PCR analysis was carried out to quantify the inversion efficiency of *Ura/Leu* cassette.

Growth curve assay

The single colony was cultured to saturation in 5 mL liquid medium SC-URA-HIS at 30°C on a rotary shaker (220 rpm). Cultures were inoculated from 24-h precultures, at an initial OD_{600} of 0.1 in 50 mL liquid medium SC-URA-His and cultivated at 220 rpm, 30°C for 72 h. Spectrophotometry was used to measure the OD_{600} value at appropriate intervals.

QUANTIFICATION AND STATISTICAL ANALYSIS

Quantification of recombination efficiency

Following the recombination experiment, 96 colonies were randomly selected and spread on an SC-Leu-Ura (SC-URA) plate overnight. The deletion of efficiency characterization cassettes was quantified by counting the number of colonies which could not grow on SC-LEU-URA (SC-URA) plate (N_D). In addition, PCR and sequencing were used to verify the inversion of efficiency characterization cassettes. Colonies that could grow on the SC-LEU-URA (SC-URA) plate were resuspended in 50 μL of 20 mM NaOH. The cells were heated for 3 cycles of 95°C/5 min and 4°C/1 min prior to adding the PCR mix, and the PCR program was performed using primer JYW109 and primer JYW111. The following PCR program was used: 95°C/3 min; 35 cycles of 95°C/15 s, 55°C/15 s, and 72°C/15 s; a final extension of 72°C/5 min. PCR reaction was generated using 2× Rapid Taq Master Mix (Vazyme Biotech Co., Ltd). Agarose gel electrophoresis was used to perform the inversion event. A PCR product (471 bp) was generated only when the efficiency characterization cassettes were inverted. To quantify the efficiency of the inversion event more accurately, colonies that can generate PCR product (471 bp) were picked up to a new SC-LEU-URA (SC-URA) plate to produce single colonies for 2–3 days at 30°C. Four single colonies were randomly picked from each colony to perform the PCR program using primer JYW109 and primer JYW111. Primer JYW109 and primer JYW110 were also used to verify whether the efficiency characterization cassettes were inverted. Primers JYW109 and JYW111 were able to amplify the PCR product (471 bp), while primer JYW109 and JYW110 failed to amplify the PCR product, which was counted as one inversion event. The inversion of efficiency characterization cassettes was quantified by counting the number of inversion events (N_I). Mean values were calculated from three separate experiments to quantify the efficiency of recombination event. Deletion efficiency (E_D) and inversion efficiency (E_I) were calculated as:

$$ED = ND/96 \quad EI = NI/(4 * 96) \qquad \text{(Equation 1)}$$

Rapid quantification of recombination efficiency

Following the recombination experiment, the cells were washed three times with water before they were serially diluted and spread on the solid medium SC, SC-URA, SC-LEU and SC+G418 with the appropriate bacteria amount. Recombination efficiency was quantified by counting the number of colonies on each

plate (N_{Ura}, N_{Leu}, N_{G418}, N_{SC}). Colonies with deletion events can grow on SC+G418, while colonies with inversion events can grow on SC-LEU. In addition, colonies without recombination events can grow on SC-URA, and all colonies can grow on SC. Mean values were calculated from three separate experiments to quantify the efficiency of recombination event. Deletion efficiency (E_D) and inversion efficiency (E_I) were calculated as:

$$ED = NG418/(NUra + NLeu + NG418)\ EI = NLeu/(NUra + NLeu + NG418) \quad \text{(Equation 2)}$$